Photosensitizing Activity of Nanoparticles of Poly (2-amino phenol)/Gold for Intensified Doxorubicin Therapeutic Effect on Melanoma Cancer Cells under Synergism Effect of 808-nm Light

Naghmeh Sattarahmady (PhD)[1,2]*, Zahra Kayani (PhD)[1,3], Hossein Heli (PhD)[1], Parsa Faghani-Eskandarkolaei (MSc Student)[2], Hanieh Haghighi (MSc)[1,2]

[1]Nanomedicine and Nanobiology Research Center, Shiraz University of Medical Sciences, Shiraz, Iran
[2]Department of Medical Physics and Engineering, School of Medicine, Shiraz University of Medical Sciences, Shiraz, Iran
[3]Research Center for the Physics of Matter and Radiation, Namur Research Institute for Life Sciences, University of Namur, Belgium

ABSTRACT

Background: Photothermal therapy (PTT) is one of the effective and non-invasive strategies which hold great promise for improving the treatment of cancer cells. PTT is based on activating a photosensitizer by infrared light irradiation and producing heat and reactive species and apoptosis in the tumor area.

Objective: The aim of this study was to investigate the effect of photothermal/chemotherapy on melanoma cancer cells using poly (2-amino phenol)/gold (P2AO/AuNPs) and doxorubicin (DOX).

Material and Methods: In this experimental study, nanoparticles of P2AO/AuNPs were synthesized, and their mixture with DOX was applied as a photosensitizer for photothermal/chemotherapy of a C540 (B16-F10) melanoma cell line.

Results: P2AO/AuNPs generated heat and cytotoxic responsive oxygen species (ROS) upon 808-nm light irradiation with simultaneous intensifying DOX therapeutic effect under domination of synergism effects between light irradiation, P2AO/AuNPs, and doxorubicin. Cell treatment with both P2AO/AuNPs and DOX resulted in a considerable increase in necroptotic cells to 61% with a significant decrease in the living cells (39%).

Conclusion: P2AO/AuNPs provided a platform for light absorption and intensifying DOX therapeutic effect. This study approved the applicability of a new photothermal/chemotherapy by domination of synergistic effects attained by combination of laser light, P2AO, AuNPs, and DOX.

Citation: Sattarahmady N, Kayani Z, Heli H, Faghani-Eskandarkolaei P, Haghighi H. Photosensitizing Activity of Nanoparticles of Poly (2-amino phenol)/Gold for Intensified Doxorubicin Therapeutic Effect on Melanoma Cancer Cells under Synergism Effect of 808-nm Light. *J Biomed Phys Eng*. 2024;14(6):547-560. doi: 10.31661/jbpe.v0i0.2312-1693.

Keywords

Metal Nanoparticles; Phototherapy; Malignant Melanoma; Photoablation; Apoptosis; Doxorubicin

Introduction

These days, melanoma, a malignant conversion of melanin-producing cells, is presented as one of the most aggressive and metastatic skin cancers [1, 2]. While ordinary disease treatment experiences low accuracy, high risks, and troublesome reactions in healthy cells, improvement of sheltered, viable and helpful modalities with moderated antagonistic impacts is significant in melanoma cancer

*Corresponding author:
Naghmeh Sattarahmady
Nanomedicine and Nanobiology Research Center, Shiraz University of Medical Sciences, Shiraz, Iran
E-mail: sattarahmady@yahoo.com

Received: 5 December 2023
Accepted: 23 February 2024

treatment. Today, we look for rational treatments with the least amount of invasion and best results.

Photothermal (PTT) and photodynamic (PDT) therapies are groundbreaking therapeutic modalities that leverage nanotechnology and light-based interventions to address the limitations of conventional melanoma treatments [3-5]. Nano systems enhance treatment outcomes by protecting sensitive therapeutic agents, optimizing pharmacokinetics, increasing bioavailability, and serving as carriers for natural compounds, drugs, and genes or acting directly as anti-melanoma agents [5]. The success of nanomedicine is evident in the approval and ongoing clinical trials of various formulations [4-6]. Activation by external stimuli, in PTT and PDT, underscores the versatility of nano systems in melanoma therapy. PTT and PDT utilize laser irradiation and photosensitizing agents to trigger a cascade of chemical, biological, and physiological reactions, leading to the demise of neoplastic cells. PTT is based on the conversion of visible or near-infrared (NIR) light energy into thermal energy, increase in temperature at the tumor location, and induction of apoptosis and necrosis. However, the killing mode of PDT on tumor cells is through light absorption of photosensitizer and formation of its excited singlet and triplet states that are followed by electron transfer to other molecules (such as molecular oxygen), and final reactive oxygen species (ROS) generation [5, 6]. The mechanisms include endoplasmic reticulum stress, ROS-mediated autophagy, release of damage-associated molecular patterns, and immunogenic tumor cell death [7]. Indeed, PTT and PDT, coupled with nanotechnology advancements, present a multifaceted and promising approach for melanoma treatment, addressing challenges and offering new horizons in therapeutic efficacy and safety. Although some pre-clinical investigations are being followed in the field of PTT/PDT in a wide range of cancers, including melanoma, there are still outstanding issues which should be clarified in future studies regarding the approval of these modalities in melanoma cancer treatment. Ongoing research in Nano systems, immunomodulation, and combination therapies continue to drive innovation in the field [5].

Among a variety of NIR photothermal transducers, gold nanoparticles (AuNPs) have critical functions including surface plasmon resonance (SPR) activity to convert the NIR light into local heat, size ward shading, biocompatibility, low toxicity, and simple surface functionalization [8]. Therefore, it is expected to achieve advanced anti-cancer property by combining PTT and chemotherapeutic drugs based on AuNPs as a photosensitizer. Up to now, researchers have orchestrated different sorts of AuNPs with various properties of continuous imaging, and photothermal/photodynamic and nanozyme oxidative treatments [9]. Synergistic PTT/chemotherapy of 4T1 cells using AuNPs coupled with metformin [10], mesoporous silica-coated gold nanorods for gene/immunotherapy of MC38 cells [11], green synthesized AuNPs for PTT of basal cell carcinoma [12], PTT of Colorectal Cancer in a Mouse Model using gold nanoshells-combined liposomal doxorubicin (DOX) [13], a series of thiol-terminated PEG-paclitaxel derivatives-conjugated AuNPs [14] and multifunctional gold-DOX nanoparticles system for pH-triggered intracellular anticancer drug release, and provision of a promising platform for intracellular delivery of a variety of anticancer drugs [15] have been the routes for PTT/chemotherapy of cancer.

Recently, conducting polymers is being considered for a range of biomedical applications, including the development of artificial muscle [16], controlled drug release [17], stimulation of nerve regeneration [18] and biosensing [19-21]. Low cytotoxicity and high

biocompatibility of these materials are evident from the growth of cells in conducting polymers and for indicating small degree of inflammation in test animals for several weeks [22]. Conducting polymers are redox-active with the potential to act as reducing agents and scavengers of free radicals. However, their antioxidant ability in biological media needs to be examined to assess their likely activities in biomedical applications [23]. A review of literature indicated that certain polymeric carriers by inhibiting the P-glycoprotein (P-gp) drug efflux system will sensitize drug-resistant cells to a group of cytotoxic drugs [24-26]. This would increase intracellular concentration of intracellular drug to the concentrations required for induction of cytotoxicity [27, 28].

Based on a literature review, some studies have been carried out for applications of poly (2-amino phenol) (P2AO) in drug sensing [20], biosensing [21], antibacterial composites [29], biomimetic coatings [30] and protein-repellence membranes [31]. However, no attempt was made for synthesis of nanoparticles of (P2AO)/gold (P2AO/AuNPs) as a photosensitizer as well as DOX intensifier in a synergistic manner for melanoma cancer cells killing.

Material and Methods

Materials

In this experimental study, all chemicals were obtained from Sigma Chemicals Co. (USA), Scharlau Chemie Co. (Spain), or Merck Co. (Germany), and used without further purification. Before use, all glassware was washed with fresh aqua regia and then deionized (DI) water. DI water was used throughout the experiments.

A C540 (B16-F10) cell line derived from mouse malignant melanoma was prepared from Pasteur Institute of Iran. The cells were cultured in Roswell Park Memorial Institute-1640 (RPMI) medium, which contained 1% antibiotics (penicillin-streptomycin, 10,000 µg mL^{-1}) and 10% fetal bovine serum (FBS) in a humidified atmosphere comprising 5% CO_2 at 37 °C. Cell incubator conditions of 5% CO_2 at 37 °C were followed throughout the study.

Synthesis and characterization of P2AO/AuNPs and P2AO/AuNPs-DOX mixture (P2AO/AuNPs-DOX)

Firstly, AuNPs were prepared by the citrate method, as described previously [32, 33]. Chloroauric acid (250 mL, 1.0 mmol L^{-1}) was mixed with sodium citrate (25 mL, 39 mmol L^{-1}), and the resultant mixture was boiled in a glass round bottom flask in a reflux equipment for 15 min. The resultant AuNPs solution was then cooled to room temperature. Then, into 4.5 mL AuNPs solution of 13.3 nmol L^{-1}, 300 µL sodium dodecyl sulfate solution of 40 mmol L^{-1} and 1.5 mL 2-aminophenol solution of 2.0 mmol L^{-1} were added. The resultant solution was mixed by a vortex mixture for one minute followed by addition of 1.5 mL acidic ammonium persulfate solution of 2 mmol L^{-1} in 10 mmol L^{-1} hydrochloric acid. After mixing again for one minute, the obtained solution was mixed by a stirrer for 4 h. The obtained P2AO/AuNPs were washed three times by DI water.

Zeta potential, size, and morphology of P2AO/AuNPs were evaluated by a SZ-100 HORIBA zeta potentiometer (Japan) and a Zeiss, TESCAN Mira 3-XMU field emission scanning electron microscope (FESEM, Czech Republic).

Laser instrument

A diode laser system from Thorlabs (Germany) working at 808 nm with an optical output power of 1000 mW with a bench top temperature controller was used. Output power density of the diode laser was fixed at 1.0 W cm^{-2} by changing the spot size of the output mounting lens and the distance between the

lens and the target. Irradiation was performed over the 96-well culture plates for 10 min.

Temperature changes of P2AO/AuNPs upon laser light irradiation

A digital thermoprobe of Lutron (Taiwan) with precision of 0.01 °C was placed in the center of the glass cuvette contained P2AO/AuNPs suspension (50 µg mL^{-1}) to measure temperature changes upon laser irradiation. P2AO/AuNPs suspension were irradiated by an 808-nm diode laser 1.0 W cm^{-2} and temperature was recorded after 10 min.

In vitro cytotoxicity evaluation of P2AO/AuNPs, DOX and P2AO/AuNPs-DOX

In vitro toxicity effect of P2AO/AuNPs, DOX, and P2AO/AuNPs-DOX on the C540 cells was measured using the MTT (3-(4,5-dimethylthiazol-2-yl)-2,5-diphenyl-tetrazolium bromide assay. 24-h cultured C540 cells in the culture plates (5.0×10^4 cells $well^{-1}$) were treated with different concentrations of P2AO/AuNPs: 0 (Ctrl), 10 (N10), 50 (N50), 100 (N100) and 250 (N250) µg mL^{-1}, DOX: 0 (Ctrl), 0.15 (D0.15), 0.3 (D0.3), 1.0 (D1) and 3.0 (D3) µg mL^{-1}, or P2AO/AuNPs-DOX with different contents of the components of P2AO/AuNPs: 50 µg mL^{-1}+DOX: 0 µg mL^{-1} (N50), P2AO/AuNPs: 50 µg mL^{-1}+DOX: 0.15 µg mL^{-1} (N50+D0.15), P2AO/AuNPs: 50 µg mL^{-1}+DOX: 0.3 µg mL^{-1} (N50+D0.3), P2AO/AuNPs: 50 µg mL^{-1}+DOX: 1.0 µg mL^{-1} (N50+D1), P2AO/AuNPs: 50 µg mL^{-1}+DOX: 3.0 µg mL^{-1} (N50+D3), P2AO/AuNPs: 50 µg mL^{-1}+DOX: 0 µg mL^{-1} (N100), P2AO/AuNPs: 100 µg mL^{-1}+DOX: 0.15 µg mL^{-1} (N100+D0.15), P2AO/AuNPs: 100 µg mL^{-1}+DOX: 0.3 µg mL^{-1} (N100+D0.3), P2AO/AuNPs: 100 µg mL^{-1}+DOX: 1.0 µg mL^{-1} (N100+D1), and P2AO/AuNPs: 100 µg mL^{-1}+DOX: 3.0 µg mL^{-1} (N100+D3), for 4 h. Then, the cell media were rinsed and refreshed with fresh medium culture, followed by incubation overnight in a humidified atmosphere comprising 5% CO_2 at 37 °C. The cytotoxicity was then measured by the by the 3-(4,5-dimethylthiazol-2-yl)-2,5-diphenyltetrazolium bromide (MTT) assay. For this assay, the wells medium was washed with 100 mmol L^{-1} phosphate buffer saline (PBS) three times, substituted with 100 µL of a MTT solution of 0.5 mg mL^{-1} dissolved in PBS, and finally incubated for 4 h at 37 °C. Afterward, the plates were centrifuged and the wells medium was substituted with 100 µL of dimethyl sulfoxide to dissolve the MTT formazan crystals. The optical intensity of each well was recorded at 570 nm using a microplate reader of Stat Fax (USA). Cytotoxicity values were reported as the ratio of absorbance of each well and control. All measurements were performed in triplicate.

In vitro cytotoxicity evaluation of P2AO/AuNPs, DOX, and P2AO/AuNPs-DOX upon laser light irradiation

In vitro photosensitizing effect of P2AO/AuNPs, DOX, and P2AO/AuNPs-DOX on C540 cells was investigated by cytotoxicity evaluation using the MTT assay upon laser light irradiation. 24-h cultured C540 cells in the culture plates (5.0×10^4 cells $well^{-1}$) in RPMI medium, which contains 1% antibiotics (penicillin-streptomycin, 10,000 µg mL^{-1}); also, 10% FBS were treated with different concentrations of P2AO/AuNPs: 0 (Ctrl), 10 (N10), 50 (N50), 100 (N100) and 250 (N250) µg mL^{-1}, DOX: 1.0 µmol L^{-1} (D1) and P2AO/AuNPs-DOX of P2AO/AuNPs: 50 µg mL^{-1}+DOX: 1.0 µmol L^{-1} (N50+D1) for 4 h. Then, the cell media were rinsed and refreshed with fresh medium culture, followed by laser light irradiation. After irradiation, the cells were incubated overnight in a humidified atmosphere comprising 5% CO_2 at 37 °C. Cells without any treatment were considered as controls.

Domination of any synergism effect between laser light irradiation and P2AO/

AuNPs, DOX, or P2AO/AuNPs-DOX to cell killing was inspected by calculation of combination indices (CIs). CI is represented as [34]:

$$CI=V_A\times V_B/V_{AB} \qquad (1)$$

Where V_A, V_B, and V_{AB} are the cell viabilities under effects of A, B (alone) and their combination, respectively. For, CI>1, CI=1, or CI<1, domination of synergism, additive or antagonism effects of A and B agents, respectively, is witnessed.

Detection of intracellular generation of ROS

As a signal of intracellular ROS production, intensity of fluorescence emission of 2′,7′-dichlorodihydrofluorescein diacetate (H2DCF-DA) was measured. The cells were seeded in 96-well plates at a density of (1×10^5 cells $well^{-1}$) in RPMI medium, which contains 1% antibiotics (penicillin-streptomycin, 10,000 µg mL^{-1}) and 10% FBS, and prepared according to the procedure mentioned in sections 2.5 with the difference that after 3.5 h of incubation, the cells were treated by 100 µL of a fresh H2DCF-DA solution (50 µmol L^{-1}) followed by incubation continuation for 30 min. Then, laser light was the irradiation used in the related cells, and after 30 min, the extracellular H2DCF-DA was rinsed thrice with PBS; ultimately, 100 mL of a lysis buffer (containing 0.1% triton X-100, 150 mmol L^{-1} NaCl, 50 mmol L^{-1} Tris-HCl buffer, pH=8.0) was added into each well. The intensity of fluorescence emission at 520 nm was measured upon excitation at 485 nm in black plates using a microplate reader of Biotek (USA).

Apoptosis assay

Apoptosis was evaluated by fluorescence-activated cell sorting (FACS analysis), using Annexin V-FITC/PI staining kit from BD Pharmingen (USA). The C540 cells were seeded in 12-well plates at a density of 1×10^5 cells $well^{-1}$ and prepared according to the procedure mentioned in sections 2.5. After 24 h of incubation, the cells were harvested, washed with PBS, and stained with Annexin V-FITC (5 µL) and propidium iodide (5 µL), followed by flowcytometry analysis by BD FACSCalibur (USA). The apoptosis rate was evaluated based on the fluorescence of 10,000 events.

In vitro evaluation of P2AO/AuNPs uptake using inductively coupled plasma optical emission spectrometry (ICP-OES)

For determination of the uptake quantity of P2AO/AuNPs by C540 cells cultured in RPMI medium, which contains 1% antibiotics (penicillin-streptomycin, 10,000 µg mL^{-1}) and 10% FBS, 24-h post-seeding cells were treated with P2AO/AuNPs. Then, they were washed with PBS thrice and lysed and digested with aqua regia. Gold content of the cells was determined using a Varian 730-ES ICP-OES (USA) in peak hopping gas mode.

Statistical analysis

For each determination, a minimum of three parallel measurements were done, and final values were expressed as mean±standard deviation. Non-parametric Kruskal-Wallis- and T-tests were employed for the analysis of statistical significance of the values using the Prism 6 software. *P*-values less than 0.05 were considered statistically significant.

Results

Although new drugs and expectations have arisen for patients with melanoma in recent years, it is generally still incurable over the last 30 years. The new discovered PTT has the potential to treat this type of cancer in some stages and prolong the patient's life and can shrink the tumor and relieve symptoms. PTT is not as aggressive as conventional chemotherapy because plasmonic AuNPs used which can absorb light at specific wavelengths

result in hyperthermic cancer treatments. It would be expected that P2AP with biocompatibility and low cytotoxicity can extend the blood half-life of P2AO/AuNPs, enhance cellular uptake, and reduce non-specific protein adsorption to some extent. We made an attempt to introduce P2AO/AuNPs-DOX as a dual therapy including photothermal therapy and chemotherapy in a synergistic manner working at reduced concentrations of both the photosensitizer and drug.

Morphology and size of P2AO/AuNPs were inspected by FESEM. A typical FESEM image of P2AO/AuNPs is presented in Figure 1. The FESEM image showed that P2AO/AuNPs consisted of spherical gold nanoparticles covered with an amorphous layer of P2AP which were connected together. The average size of P2AO/AuNPs was 9.5±5 nm. Particle size analysis by dynamic light scattering for Au@POAP NPs (Figure 2) showed hydrodynamic diameter of 11±4 nm, with a polydispersity index of 0.5. Zeta potential of P2AO/AuNPs was also measured to be -0.5 mV.

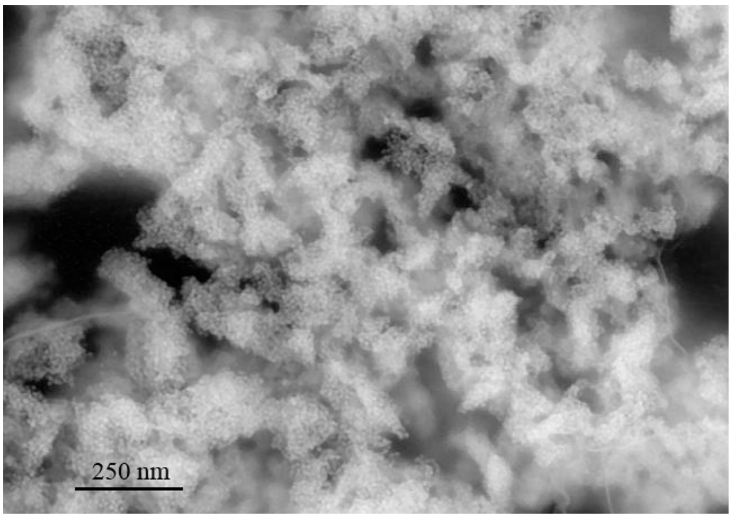

Figure 1: A Field emission scanning electron microscopy (FESEM) image of P2AO/AuNPs. The image consisted of spherical gold nanoparticles covered with an amorphous layer of P2AP

To evaluate the photothermal effect of P2AO/AuNPs, their temperature increment at concentration of 50 µg mL^{-1} was measured under 808-nm irradiation at a power density of 1 W cm^{-2} for 10 min and a temperature increment of 5.32 °C was recorded.

Figure 3 shows cytotoxicity effects of P2AO/AuNPs, DOX, and P2AO/AuNPs-DOX toward C540 cells evaluated by the MTT assay. The results of cytotoxicity of different concentrations indicated that P2AO/AuNPs had

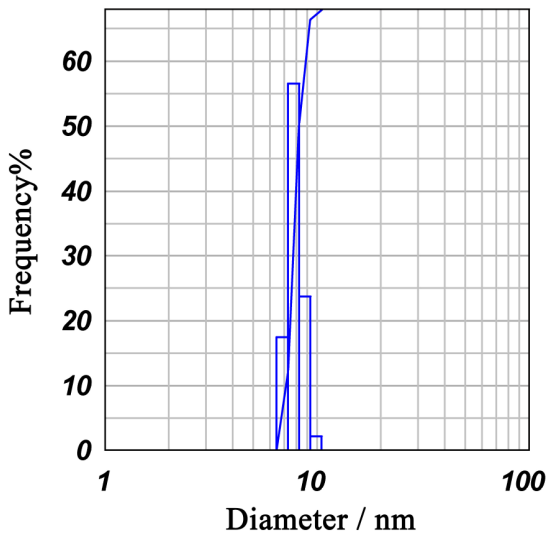

Figure 2: Particle size analysis of Au@POAP NPs by dynamic light scattering. Au@POAP nanoparticles showed hydrodynamic diameter of 11±4 nm, with a polydispersity index of 0.5

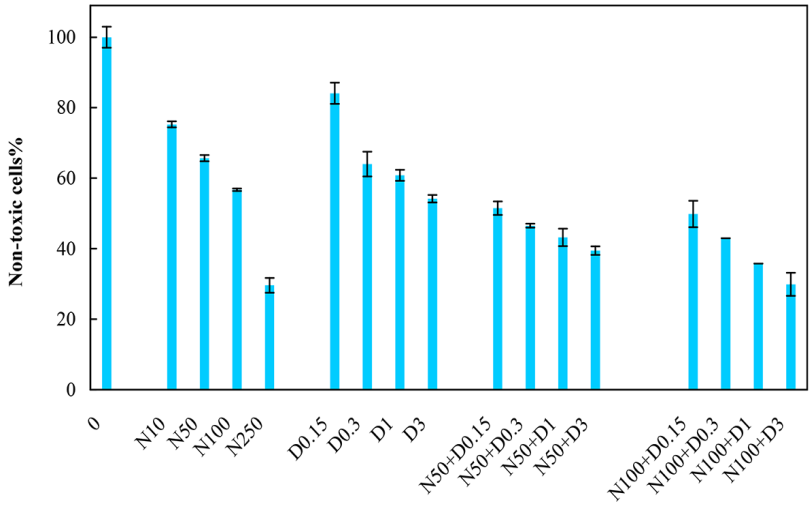

Figure 3: Cytotoxicity effects of P2AO/AuNPs, DOX and Au@POAP NPs +DOX toward C540 cells. Different concentrations of P2AO/AuNPs (0, 10 (N10), 50 (N50), 100 (N100) and 250 µg mL^{-1} (N250)), DOX (0.15 (D0.15), 0.3 (D0.3), 1.0 (D1) and 3.0 µmol L^{-1} (D3)), and P2AO/AuNPs-DOX (Au@POAP NPs of 50 µg mL^{-1}+DOX of 0.15, 0.3, 1.0 and 3.0 µmol L^{-1} (N50+D0.15, N50+D0.3, N50+D1 and N50+D3), and Au@POAP NPs of 100 µg mL^{-1}+DOX (0.15, 0.3, 1.0 and 3.0 µmol L^{-1} (N100+D0.15, N100+D0.3, N100+D1 and N100+D3)) was evaluated by the MTT assay

a relative toxicity (cell viability >56% in the presence of 10, 50 and 100 µg mL^{-1}, and ~29% in the presence of 250 µg mL^{-1}) with an estimated half-maximal inhibitory concentration (IC50) of 140 µg mL^{-1}. Cytotoxicity of different concentrations of DOX also resulted in an IC50 of ~4.6 µmol mL^{-1}. Combination of a fixed amount of P2AO/AuNPs of 50 µg mL^{-1} with various concentrations of DOX (0.15, 0.3, 1.0 and 3.0 µmol mL^{-1}) led to a decreased IC50 of ~0.17 µmol mL^{-1} for DOX. Moreover, combination of P2AO/AuNPs of 50 µg mL^{-1}) with various concentrations of DOX (0.15, 0.3, 1.0 and 3.0 µmol mL^{-1}) led to a decreased IC50 of ~0.10 µmol mL^{-1} for DOX.

Figure 4 shows cytotoxicity effects of P2AO/AuNPs and P2AO/AuNPs-DOX upon laser light irradiation toward C540 cells evaluated by the MTT assay. The results showed a cell viability of 91% upon laser light irradiation, indicating that the irradiation had a non-toxic effect. However, laser light irradiation of P2AO/AuNPs induced cell toxicities more that treatment with irradiation or

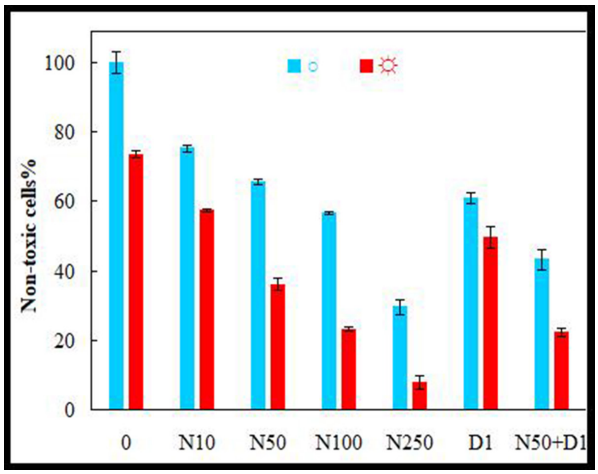

Figure 4: Cytotoxicity effects of P2AO/AuNPs, DOX and Au@POAP NPs+DOX without (○) and with laser light irradiation (☼) toward C540 cells. Different concentrations of P2AO/AuNPs (0, 10 (N10), 50 (N50), 100 (N100) and 250 µg mL^{-1} (N250)), and DOX (1.0 µmol L^{-1} (D1)), P2AO/AuNPs-DOX (Au@POAP NPs of 50 µg mL^{-1}+DOX of 1.0 µmol L^{-1}(N50+D1)), without (○) and with laser light irradiation (☼) was evaluated by the MTT assay

P2AO/AuNPs alone, and the viability values went through CIs>1. CIs for all the combination treatments are presented in Table 1. The results showed that laser light irradiation of DOX represented an additive effect arising from the effects of irradiation and the drug separately. Also, while P2AO/AuNPs had lower toxicity than DOX, laser light irradiation induced higher cell killing ability of P2AO/AuNPs than DOX. This further confirmed the photosensitizing ability of P2AO/AuNPs. In addition, cell treatment with P2AO/AuNPs-DOX, either with or without laser light irradiation, represented additive effects, when compared to treatment with P2AO/AuNPs or DOX alone. However, when laser light irradiation and treatment with P2AO/AuNPs-DOX of the cells were considered as two independent parameters, the results indicated domination of a synergistic effect for PTT, using P2AO/AuNPs-DOX. Regarding the C540 cellular uptake of P2AO/AuNPs during 4 h of incubation time, a value of 4.47 ng $cell^{-1}$ was obtained.

Intracellular ROS generation during PTT treatment of C540 cells was evaluated using the intensity of fluorescence emission of H2DCF-DA. H2DCF-DA passively penetrates the cells, and it is deacetylated by esterases to non-fluorescent H2DCF. Intracellular ROS interacts with H2DCF and produces fluorescent DCF. Figure 5 shows the intensities of fluorescence emission at 520 nm arising from intracellular ROS generation upon C540 cell treatment with P2AO/AuNPs, DOX, and P2AO/AuNPs-DOX, either with or without laser light irradiation, while the intensity of fluorescence emission of the control cells was considered as a base signal. Without laser light irradiation, the results and a comparison with those presented for cytotoxicity effects indicated that the generated ROS levels for cell treatment with P2AO/AuNPs and DOX, as presented in Figure 5, were in disagreement with the corresponding results presented in Figures 3 and 4; while ROS level for treatment with P2AO/AuNPs was greater than DOX, cell killing ability of DOX was better. The quantities of generated ROS also indicated that P2AO/AuNPs and DOX could play a synergistic role to generate ROS, either with or without laser light irradiation.

Table 1: Combination indexes (CIs) values for all the combination treatments.

Group	CI	Action
N10+L	0.96	Antagonism
N50+L	1.34	Synergism
N100+L	1.80	Synergism
N250+L	2.84	Synergism
D1+L	1.12	Synergism
N50+D1+L	1.79	Synergism

CI: Combination Index

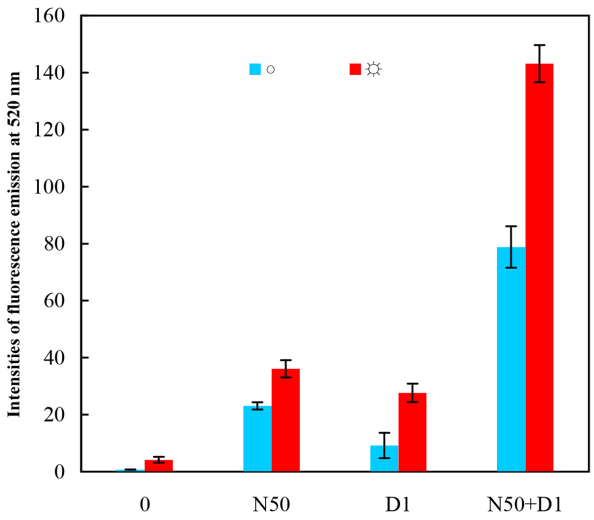

Figure 5: The impact of NIR on ROS production in C540 cells treated with P2AO/AuNPs. Intensities of fluorescence emission at 520 nm arising from intracellular ROS generation upon C540 cell treatment with P2AO/AuNPs (50 µg mL^{-1} (N50)), DOX (1.0 µmol L^{-1} (D1)) and P2AO/AuNPs-DOX (Au@POAP NPs of 50 µg mL^{-1}+DOX of 1.0 µmol L^{-1} (N50+D1)), without (○) and with laser light irradiation (☼)

Laser light irradiation of P2AO/AuNPs-DOX produced the highest ROS level.

Figure 6A shows the occurrence of apoptosis in the C540 cells upon PTT was evaluated by FACS analysis; scatter plots containing Q1 to Q4 areas indicate necrotic, late apoptotic, early apoptotic, and live cells, respectively, so that the sum of Q1, Q2 and Q3 was considered as necroptotic. Figure 6B and C show population of different cells upon treatments. Without laser light irradiation, the controls showed an insignificant number of cells in necroptotic stages (7%) with 93% of live cells. Cell treatment with P2AO/AuNPs resulted in an insignificant increase in the necroptotic cells (16%) with slight decrease in the percentage of live cells (84%). Cell treatment with DOX resulted in necroptotic population of 27%. Cell treatment with P2AO/AuNPs-DOX resulted in moderate increase in necroptotic population percentage of 48%. Laser light irradiation alone also resulted in a slight increase in the necroptotic cells (15%) and a slight decrease in live cells (85%). With laser light irradiation, cell treatment with P2AO/AuNPs and DOX resulted in moderate increase in necroptotic cells with 46 and 31%, respectively. Cell treatment with P2AO/AuNPs-DOX, however, resulted in a considerable increase in necroptotic cells to 61% with a significant decrease in the live cells (39%).

Discussion

The size, relatively uniform size distribution, and zeta potential of P2AO/AuNPs show that it can directly and effectively penetrate the cancer cells and tumor tissues; among other things, due to its small size, it can be removed from the body faster through renal filtration [35, 36].

Cytotoxicity assessment and IC50 determination indicated that combination of P2AO/AuNPs with DOX resulted in better efficiency of DOX as chemotherapy agent on melanoma cancer and very low concentration of DOX in this combination needs for killing melanoma cancer cells. Therefore, combination of P2AO/AuNPs with DOX resulted in decreased consumption of the drug to attain similar cell toxicity obtained with higher doses. Laser light irradiation at 808 nm at 1.0 W cm^{-2} power density of P2AO/AuNPs killed the cells in a synergistic manner at all the P2AO/AuNPs concentrations. However, the results confirmed that laser light irradiation had further effect on DOX cytotoxicity. Therefore, P2AO/AuNPs had lower toxicity than DOX; laser light irradiation induced higher cell killing ability of P2AO/AuNPs than DOX. This further confirmed the photosensitizing ability of P2AO/AuNPs, and synergism behavior of P2AO/AuNPs-DOX upon laser light irradiation indicated that P2AO/AuNPs uptake in cells absorbed 808-nm light to generate heat on one hand and accelerated DOX affection upon light irradiation. The light of 700- to 1000-nm is a preferable source of energy for cancer cell treatment because it is not absorbed by proteins and DNA and has a deep penetration in tissues [37]. The order of more intracellular ROS generation occurred in the presence of P2AO/AuNPs-DOX, P2AO/AuNPs, and then DOX upon laser light irradiation. While cell killing ability of DOX was better, the results of intracellular ROS indicated that the routes of cell killing of P2AO/AuNPs and DOX were different, and that for P2AO/AuNPs it was mainly based on ROS generation. Also, synergistic effects arising from combinations of P2AO/AuNPs and DOX, P2AO/AuNPs and light irradiation, and DOX and light irradiation induced ROS generation. While chemotherapy of melanoma cells with DOX induced less killing via necroptotic, its combination in P2AO/AuNPs-DOX upon laser light irradiation resulted in significant cell loss via necroptotic.

C540 cells PTT using P2AO/AuNPs-DOX

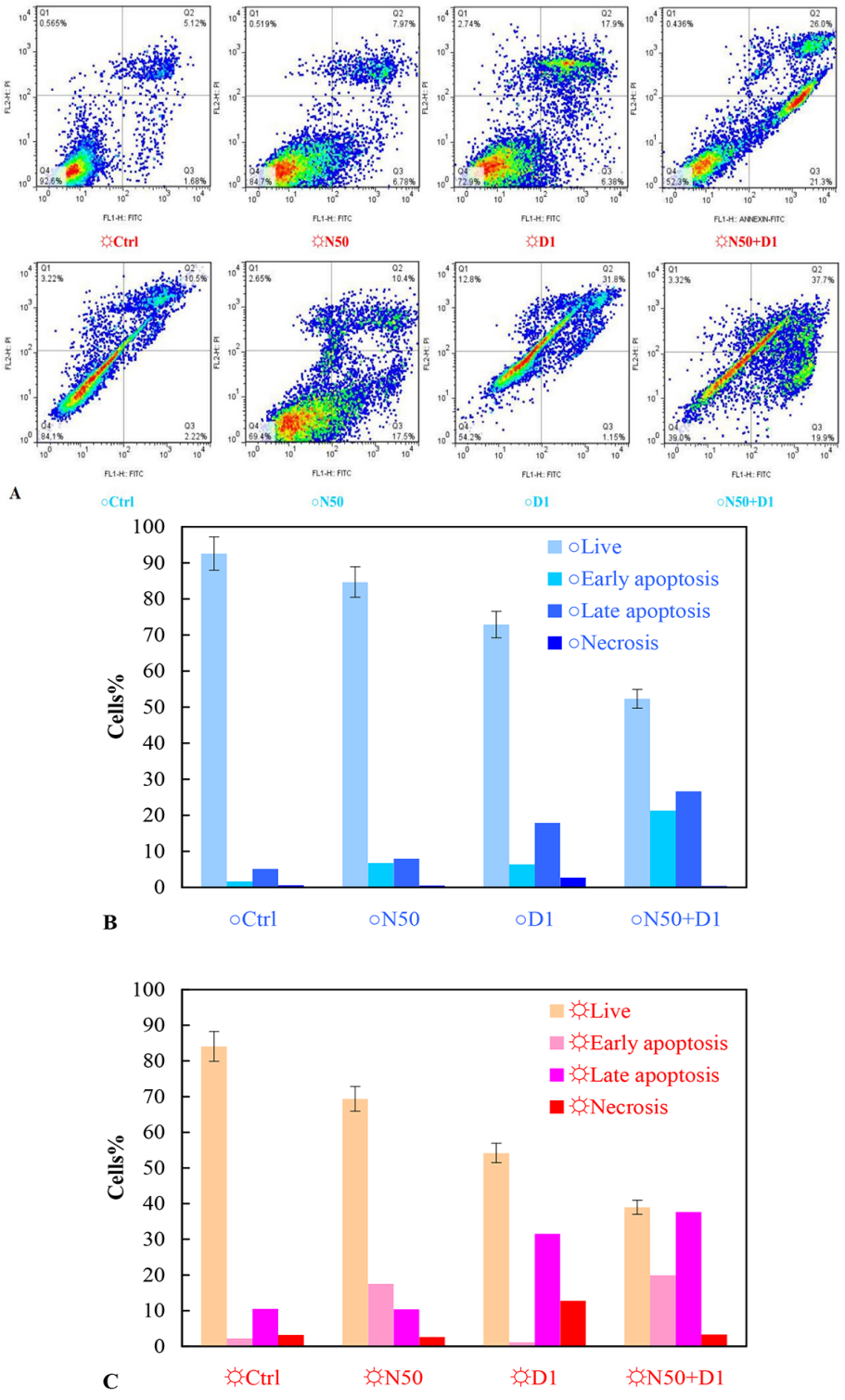

Figure 6: A: Evaluation of the apoptotic effect induced by P2AO/AuNPs in C540 cells. FACS analysis results as scatter plots for treatment of C540 cells with P2AO/AuNPs (50 µg mL^{-1} (N50)), DOX (1.0 µmol L^{-1} (D1)) and P2AO/AuNPs-DOX (Au@POAP NPs of 50 µg mL^{-1}+DOX of 1.0 µmol L^{-1} (N50+D1)), without (○) and with laser light irradiation (☼). **B, C:** Quantitative assessment of apoptotic responses in C540 cells induced by P2AO/AuNPs. Percentages of viability of live, early apoptotic, late apoptotic and necrotic C540 cells

works with three different paths: i) generates a hyperthermal microenvironment leading to induction of necrosis and/or apoptosis, ii) retards the repair of DNA damage induced with AuNPs [38, 39], and iii) intercalation of DOX into DNA and disruption of topoisomerase-II-mediated DNA repair. This study supports the idea that P2AO/AuNPs-DOX provides a good laser-responsive activity with milder chemotherapeutic conditions.

However, as with many studies, the design of the current study would be followed by in vivo investigations and clinical trials, both of which being essential for converting research results from laboratories into useful medicinal uses. Future research can also explore the effectiveness of P2AO/AuNPs in various melanoma subtypes or other types of cancers.

Conclusion

In this study, a photothermal therapy using P2AO/AuNPs was developed based on 808-nm light absorbing of both P2AO and AuNPs and energy conversion preliminary into heat. The photosensitizer P2AO/AuNPs and laser light killed C540 cancer cells through heat and ROS generation. We showed that P2AO coating of AuNPs provided a suitable platform to carry DOX, and light irradiation of P2AO/AuNPs-DOX led to intensifying DOX therapeutic effect. The employed components provided a new photothermal/chemotherapy by domination of synergistic effects attained by combination of laser light, P2AO, AuNPs, and DOX. Generation of hyperthermal microenvironment upon light irradiation of both P2AO and AuNPs, retardation of DNA damage repairing by AuNPs and DOX, and disrupting the structure of DNA led to intensifying DOX efficacy.

Although PTT holds promise in its selectivity and reduced invasiveness compared to conventional therapies, currently, using the results of this research in vivo is facing challenges. Continuous NIR energy could lead to overheating, thermal injury, inflammation, and uncomfortable and pain for patients. Moreover, challenges in intracellular delivery of P2AO/AuNPs pose additional concerns. Large tumors often feature hypoxic regions with limited blood flow and high interstitial pressure, retarding effective NP delivery. This unequal distribution and restricted laser depth induce heterogeneous heat dispersal in tumor during PTT, reducing treatment effectiveness and complicating simultaneous cancer cell eradication. Therefore, it is necessary to consider the limitations of the present research and seek a solution and opportunities for future research.

Acknowledgment

We would like to thank the Research Council of Shiraz University of Medical Sciences for supporting this research.

Authors' Contribution

Regarding the authors' contributions, N. Sattarahmady and Z. Kayani contributed to the study conception and design. N. Sattarahmady conceived the original idea and H. Heli supervised the project. Z. Kayani played a pivotal role in designing the procedure and fabrication of the nanoparticles. Material preparation, data collection, and analysis were performed by Z. Kayani, P. Faghani-Eskandarkolaei, and H. Haghighi. All authors actively contributed in writing and reviewing the manuscript, ensuring a comprehensive and well-rounded study. All authors read, modified, and approved the final version of the manuscript.

Ethical Approval

The national ethics committee confirmed the study with the ethical code of IR.SUMS.REC.1398.1179. We did not perform any intervention in therapeutic procedures. Therefore, gathering the consent forms was waived due to the nature of this study.

Funding

This work was supported by Shiraz University of Medical Sciences (Shiraz, Iran) with the grant number of "18253".

Conflict of Interest

None

References

1. Castro-Pérez E, Singh M, Sadangi S, Mela-Sánchez C, Setaluri V. Connecting the dots: Melanoma cell of origin, tumor cell plasticity, transdifferentiation, and drug resistance. *Pigment Cell Melanoma Res.* 2023;**36**(5):330-47. doi: 10.1111/pcmr.13092. PubMed PMID: 37132530. PubMed PMCID: PMC10524512.
2. Dos Reis FD, Jerónimo C, Correia MP. Epigenetic modulation and prostate cancer: Paving the way for NK cell anti-tumor immunity. *Front Immunol.* 2023;**14**:1152572. doi: 10.3389/fimmu.2023.1152572. PubMed PMID: 37090711. PubMed PMCID: PMC10113550.
3. Al-Thubiani W. The Role of P-Glycoprotein (P-gp) in Cancer Multidrug Resistance (MDR): Challenges for Inhibiting P-gp in the Context of Overcoming MDR. *J Pharm Res Int.* 2023;**35**(23):44-58. doi: 10.9734/jpri/2023/v35i237422.
4. Wang J, Wu SG. Breast Cancer: An Overview of Current Therapeutic Strategies, Challenge, and Perspectives. *Breast Cancer (Dove Med Press).* 2023;**15**:721-30. doi: 10.2147/BCTT.S432526. PubMed PMID: 37881514. PubMed PMCID: PMC10596062.
5. Lopes J, Rodrigues CMP, Gaspar MM, Reis CP. How to Treat Melanoma? The Current Status of Innovative Nanotechnological Strategies and the Role of Minimally Invasive Approaches like PTT and PDT. *Pharmaceutics.* 2022;**14**(9):1817. doi: 10.3390/pharmaceutics14091817. PubMed PMID: 36145569. PubMed PMCID: PMC9504126.
6. Nirmala MJ, Kizhuveetil U, Johnson A, G Balaji, Nagarajan R, Muthuvijayan V. Cancer nanomedicine: a review of nano-therapeutics and challenges ahead. *RSC Adv.* 2023;**13**(13):8606-29. doi: 10.1039/d2ra07863e. PubMed PMID: 36926304. PubMed PMCID: PMC10013677.
7. Chen Y, Li H, Deng Y, Sun H, Ke X, Ci T. Near-infrared light triggered drug delivery system for higher efficacy of combined chemo-photothermal treatment. *Acta Biomater.* 2017;**51**:374-92. doi: 10.1016/j.actbio.2016.12.004. PubMed PMID: 28088668.
8. Hou YJ, Yang XX, Liu RQ, Zhao D, Guo CX, Zhu AC, et al. Pathological Mechanism of Photodynamic Therapy and Photothermal Therapy Based on Nanoparticles. *Int J Nanomedicine.* 2020;**15**:6827-38. doi: 10.2147/IJN.S269321. PubMed PMID: 32982235. PubMed PMCID: PMC7501968.
9. Zhang A, Pan S, Zhang Y, Chang J, et al. Carbon-gold hybrid nanoprobes for real-time imaging, photothermal/photodynamic and nanozyme oxidative therapy. *Theranostics.* 2019;**9**(12):3443-58. doi: 10.7150/thno.33266. PubMed PMID: 31281489. PubMed PMCID: PMC6587161.
10. Yang T, Wang H, Zhou Q, Huang W, Zhang J, Yu Y, et al. Mild chemo-photothermal synergistic therapy for tumors based on gold-nanoparticles coupled with metformin. *J ACS Appl Nano Mater.* 2023;**6**(7):5729-36. doi: 10.1021/acsanm.3c00140.
11. Li M, Yang J, Yao X, Li X, Xu Z, Tang S, et al. Multifunctional Mesoporous Silica-Coated Gold Nanorods Mediate Mild Photothermal Heating-Enhanced Gene/Immunotherapy for Colorectal Cancer. *Pharmaceutics.* 2023;**15**(3):854. doi: 10.3390/pharmaceutics15030854. PubMed PMID: 36986715. PubMed PMCID: PMC10057058.
12. Bonamy C, Pesnel S, Ben Haddada M, Gorgette O, Schmitt C, Morel AL, Sauvonnet N. Impact of Green Gold Nanoparticle Coating on Internalization, Trafficking, and Efficiency for Photothermal Therapy of Skin Cancer. *ACS Omega.* 2023;**8**(4):4092-105. doi: 10.1021/acsomega.2c07054. PubMed PMID: 36743010. PubMed PMCID: PMC9893490.
13. Simón M, Jørgensen JT, Norregaard K, Henriksen JR, Clergeaud G, Andresen TL, et al. Neoadjuvant Gold Nanoshell-Based Photothermal Therapy Combined with Liposomal Doxorubicin in a Mouse Model of Colorectal Cancer. *Int J Nanomedicine.* 2023;**18**:829-41. doi: 10.2147/IJN.S389260. PubMed PMID: 36824412. PubMed PMCID: PMC9942687.
14. Zahraie N, Perota G, Dehdari Vais R, Sattarahmady N. Simultaneous chemotherapy/sonodynamic therapy of the melanoma cancer cells using a gold-paclitaxel nanostructure. *Photodiagnosis Photodyn Ther.* 2022;**39**:102991. doi: 10.1016/j.pdpdt.2022.102991. PubMed PMID: 35779857.
15. Zhan H, Song W, Gu M, Zhao H, Liu Y, Liu B, Wang J. A New Gold Nanoparticles and Paclitaxel Co-Delivery System for Enhanced Anti-Cancer Effect Through Chemo-Photothermal Combina-

tion. *J Biomed Nanotechnol.* 2022;**18**(4):957-75. doi: 10.1166/jbn.2022.3309. PubMed PMID: 35854456.

16. Benny Mattam L, Bijoy A, Abraham Thadathil D, George L, Varghese A. Conducting polymers: a versatile material for biomedical applications. *ChemistrySelect.* 2022;**7**(42):e202201765. doi: 10.1002/slct.202201765.
17. Salari N, Faraji F, Torghabeh FM, Faraji F, Mansouri K, Abam F, et al. Polymer-based drug delivery systems for anticancer drugs: A systematic review. *Cancer Treat Res Commun.* 2022;**32**:100605. doi: 10.1016/j.ctarc.2022.100605. PubMed PMID: 35816909.
18. Stocco E, Barbon S, Emmi A, Tiengo C, Macchi V, De Caro R, Porzionato A. Bridging Gaps in Peripheral Nerves: From Current Strategies to Future Perspectives in Conduit Design. *Int J Mol Sci.* 2023;**24**(11):9170. doi: 10.3390/ijms24119170. PubMed PMID: 37298122. PubMed PMCID: PMC10252835.
19. Yazdani Z, Yadegari H, Heli H. A molecularly imprinted electrochemical nanobiosensor for prostate specific antigen determination. *Anal Biochem.* 2019;**566**:116-25. doi: 10.1016/j.ab.2018.11.020. PubMed PMID: 30472220.
20. Pishahang J, Amiri HB, Heli H. Synthesis of carbon nanoparticles-poly (ortho-aminophenol) nanocomposite and its application for electroanalysis of iodate. *J Sens Actuators B Chem.* 2018;**256**:878-87. doi: 10.1016/j.snb.2017.10.030.
21. Vais RD, Heli H, Sattarahmady N, Barazesh A. A novel and ultrasensitive label-free electrochemical DNA biosensor for Trichomonas vaginalis detection based on a nanostructured film of poly (ortho-aminophenol). *J Synth Met.* 2022;**287**:117082. doi: 10.1016/j.synthmet.2022.117082.
22. Narkar AR, Tong Z, Soman P, Henderson JH. Smart biomaterial platforms: Controlling and being controlled by cells. *Biomaterials.* 2022;**283**:121450. doi: 10.1016/j.biomaterials.2022.121450. PubMed PMID: 35247636. PubMed PMCID: PMC8977253.
23. Wang Y, Wang J, Jiao Y, Chen K, Chen T, Wu X, et al. Redox-active polyphenol nanoparticles deprive endogenous glutathione of electrons for ROS generation and tumor chemodynamic therapy. *Acta Biomater.* 2023;**172**:423-40. doi: 10.1016/j.actbio.2023.09.037. PubMed PMID: 37778486.
24. Rathod S, Desai H, Patil R, Sarolia J. Non-ionic Surfactants as a P-Glycoprotein(P-gp) Efflux Inhibitor for Optimal Drug Delivery-A Concise Outlook. *AAPS PharmSciTech.* 2022;**23**(1):55. doi: 10.1208/s12249-022-02211-1. PubMed PMID: 35043278.
25. Liyanage PY, Hettiarachchi SD, Zhou Y, Ouhtit A, Seven ES, Oztan CY, et al. Nanoparticle-mediated targeted drug delivery for breast cancer treatment. *Biochim Biophys Acta Rev Cancer.* 2019;**1871**(2):419-33. doi: 10.1016/j.bbcan.2019.04.006. PubMed PMID: 31034927. PubMed PMCID: PMC6549504.
26. Attia MS, Elsebaey MT, Yahya G, Chopra H, Marzouk MA, Yahya A, Abdelkhalek AS. Pharmaceutical polymers and P-glycoprotein: Current trends and possible outcomes in drug delivery. *J Mater Today Commun.* 2023;**34**:105318. doi: 10.1016/j.mtcomm.2023.105318.
27. Alshaer W, Alqudah DA, Wehaibi S, Abuarqoub D, Zihlif M, Hatmal MM, Awidi A. Downregulation of STAT3, β-Catenin, and Notch-1 by Single and Combinations of siRNA Treatment Enhance Chemosensitivity of Wild Type and Doxorubicin Resistant MCF7 Breast Cancer Cells to Doxorubicin. *Int J Mol Sci.* 2019;**20**(15):3696. doi: 10.3390/ijms20153696. PubMed PMID: 31357721. PubMed PMCID: PMC6696135.
28. Yalamarty SSK, Filipczak N, Li X, Pathrikar TV, Cotter C, Torchilin VP. Co-Delivery of siRNA and Chemotherapeutic Drug Using 2C5 Antibody-Targeted Dendrimer-Based Mixed Micelles for Multidrug Resistant Cancers. *Pharmaceutics.* 2022;**14**(7):1470. doi: 10.3390/pharmaceutics14071470. PubMed PMID: 35890364. PubMed PMCID: PMC9324017.
29. Boomi P, Anandha Raj J, Palaniappan SP, Poorani G, Selvam S, Gurumallesh Prabu H, et al. Improved conductivity and antibacterial activity of poly(2-aminothiophenol)-silver nanocomposite against human pathogens. *J Photochem Photobiol B.* 2018;**178**:323-9. doi: 10.1016/j.jphotobiol.2017.11.029. PubMed PMID: 29178993.
30. Ciriello R, Graziano M, Bianco G, Guerrieri A. Electrosynthesized poly (o-aminophenol) films as biomimetic coatings for dopamine detection on Pt substrates. *J Chemosensors.* 2021;**9**(10):280. doi: 10.3390/chemosensors9100280.
31. Nady N, El-Shazly AH, Soliman HMA, Kandil SH. Protein-Repellence PES Membranes Using Biografting of Ortho-aminophenol. *Polymers (Basel).* 2016;**8**(8):306. doi: 10.3390/polym8080306. PubMed PMID: 30974579. PubMed PMCID: PMC6432355.
32. Sattarahmady N, Tondro G, Gholchin M, Heli H.

Gold nanoparticles biosensor of Brucella spp. genomic DNA: Visual and spectrophotometric detections. *Biochem Eng J.* 2015;**97**:1-7. doi: 10.1016/j.bej.2015.01.010.

33. Heli H, Rahi A. Synthesis and Applications of Nanoflowers. *Recent Pat Nanotechnol.* 2016;**10**(2):86-115. doi: 10.2174/1872210510999160517102102. PubMed PMID: 27502388.
34. Ma J, Motsinger-Reif A. Current Methods for Quantifying Drug Synergism. *Proteom Bioinform.* 2019;**1**(2):43-8. PubMed PMID: 32043089. PubMed PMCID: PMC7010330.
35. Xia Q, Huang J, Feng Q, Chen X, Liu X, Li X, et al. Size- and cell type-dependent cellular uptake, cytotoxicity and in vivo distribution of gold nanoparticles. *Int J Nanomedicine*. 2019;**14**:6957-70. doi: 10.2147/IJN.S214008. PubMed PMID: 32021157. PubMed PMCID: PMC6717860.
36. Huo S, Ma H, Huang K, Liu J, Wei T, Jin S, et al. Superior penetration and retention behavior of 50 nm gold nanoparticles in tumors. *Cancer Res.* 2013;**73**(1):319-30. doi: 10.1158/0008-5472.CAN-12-2071. PubMed PMID: 23074284.
37. Lima-Sousa R, Melo BL, Alves CG, Moreira AF, Mendonça AG, Correia IJ, et al. Combining Photothermal-Photodynamic Therapy Mediated by Nanomaterials with Immune Checkpoint Blockade for Metastatic Cancer Treatment and Creation of Immune Memory. *J Adv Funct Mater.* 2021;**31**(29):2010777. doi: 10.1002/adfm.202010777.
38. Kim B-S, Kumar D, Park CH, Kim CS. HSPA1A-siRNA nucleated gold nanorods for stimulated photothermal therapy through strategic heat shock to HSP70. *J Mater Chem Front.* 2021;**5**(17):6461-70. doi: 10.1039/D1QM00630D.
39. Moros M, Lewinska A, Merola F, Ferraro P, Wnuk M, Tino A, Tortiglione C. Gold Nanorods and Nanoprisms Mediate Different Photothermal Cell Death Mechanisms In Vitro and In Vivo. *ACS Appl Mater Interfaces*. 2020;**12**(12):13718-30. doi: 10.1021/acsami.0c02022. PubMed PMID: 32134240.